Chinese Chemical Letters 33 (2022) 89–96

Contents lists available at ScienceDirect

Chinese Chemical Letters

journal homepage: www.elsevier.com/locate/cclet

The emerging applications of pillararene architectures in supramolecular catalysis

Kaiya Wang[a], Xueqi Tian[a], Jacobs H. Jordan[b], Krishnasamy Velmurugan[a], Leyong Wang[c], Xiao-Yu Hu[a,*]

[a] College of Materials Science and Technology, Nanjing University of Aeronautics and Astronautics, Nanjing 211106, China
[b] The Southern Regional Research Center, Agricultural Research Service, USDA, New Orleans, LA 70124, United States
[c] Key Laboratory of Mesoscopic Chemistry of MOE, School of Chemistry and Chemical Engineering, Nanjing University, Nanjing 210023, China

ARTICLE INFO

Article history:
Received 30 April 2021
Revised 5 June 2021
Accepted 7 June 2021
Available online 13 June 2021

Keywords:
Supramolecular catalysis
Host–guest chemistry
Macrocycles
Pillararene
Self-assembly

ABSTRACT

Over the last decade, numerous research efforts have been devoted to pillar[*n*]arenes since their debut. The popularity of pillararenes is a reflection of current research trend in supramolecular and macrocyclic chemistry in general. Among the vast applications (such as chemosensors, drug delivery, transmembrance channels, and separation) of pillararenes, their utilization in catalysis is a relatively less explored area. However, soaring attention has been paid by researchers in recent years and this field has seen gradual increasing publications. Therefore, in this review we will discuss progress in the emerging applications of pillararene architectures in catalysis based on various reaction genre including reduction, oxidation, coupling, decomposition and others. Furthermore, this review not only focuses on the pillararenes based current progress in catalysis, but also provides the signs for future development in this research field.

1. Introduction

Natural enzymes as multifunctional catalysts have constantly inspired scientists to search for their man-made counterparts [1, 2]. A key feature of enzymes is their compartmentalized nano-spaces, which are able to bind and recognize various substrates [3]. Reactions that occur in these enzymatic pockets typically feature high selectivity and rate acceleration [4]. Supramolecular chemists tend to use structures with confined cavities to mimic enzymes in order to obtain desired catalytic efficiency [5,6]. These confined nano-spaces offer many advantages for chemical reactions, such as pre-organization, intermediate or transition state stabilization, and high local concentration [7]. Over the years, a variety of supramolecular hosts have been constructed and employed as catalysts [8,9]. While great progress has been made towards duplicating enzymes' specificity, many potential challenges remain.

Pillar[*n*]arenes (PA[*n*]s, $n = 5–15$), are a new family of host molecules after crown ethers, cyclodextrins, calixarenes, and cucurbiturils [10]. PAs are *para*-bridged pillar-shaped macrocycles that are among the most fascinating and highly-studied scaffolds in supramolecular chemistry [11,12]. This stems from their facile synthesis, functional and tunable diversity at both rims, preorganized rigid shape, capacious cavities, and well-defined conformations [13]. PAs could form inclusion complexes with various guests in organic/aqueous environments. The unique structures of the PAs (symmetrical, rigid, facile (mono-/di-/per-) functionalization) contain hydrophobic inner cavity facilitate them to form inclusion complexes with target guests (charged/neutral) *via* hydrophobic, dipole-dipole, hydrogen bonding, $\pi\cdots\pi$, C-H$\cdots\pi$ interactions and their inclusion properties vary extensively. These resulting complexes are responsive to external stimuli, such as temperature, light, pH, redox, ion [14,15]. This provides the supramolecular nanostructures with responsiveness, thus could be utilized for a wide range of applications. Early research focused on PA functionalization and binding properties, which formed the foundation for their subsequent utilization. Nowadays, the PA family stands out with various promising applications in multiple fields including drug delivery, nanomaterials, sensors, transmembrance channels, and catalysis [16-22], among which, the field of catalysis is rapidly evolving and one of the fastest-growing areas.

One of the earliest examples of PAs based catalysis was developed by Ogoshi in 2013 for the phase transfer catalysis of alkene oxidation [23]. The Huang group is also among the pioneers in employing PAs based hybrid materials as catalysts for nitrobenzene reduction [24]. Subsequently, this field has attracted many

* Corresponding author.
E-mail address: huxy@nuaa.edu.cn (X.-Y. Hu).

https://doi.org/10.1016/j.cclet.2021.06.026
1001-8417/

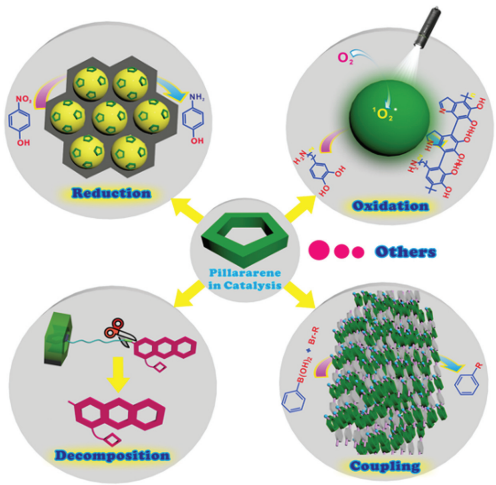

Fig. 1. Schematic representation of different varieties of reactions catalyzed by PAs based structures and materials.

researchers and the emerging applications of PAs in catalysis have developed gradually, concurrent with an increase in the fundamental understanding of host–guest and assembly properties of Pas [25-34]. PAs can function as catalysts alone, either within the cavity or by utilizing the reactive rims. Incorporation of PA scaffolds with different functionalities has led to the development of various catalytic materials. For example, PA scaffold has been playing a vital role in catalytic reactions, such as stabilizer for small size nanoparticles (NPs) formation, making close proximity between NPs and substrate in reduction reaction *via* host-guest approach, (co)catalysts for Pd-catalyzed Suzuki and Heck reactions, weak base for Knoevenagel condensation, functionalized rims with hydrophobic cavities of PA for decomposition reaction, and acting as additives in aqueous biphasic catalysis.

Thus far, there has been only one published minireview discussing different strategies in applying PAs in catalysis, while only some representative examples are included [35]. It summarizes the development of functionalized PA architectures in catalysis with topics subdivided based on rim/cavity promoted catalysis, PAs based nanomaterials, and polymeric materials. Herein, this present review aims to elucidate the important roles of PAs based architectures in catalyzing different reaction types. It is not intended to be comprehensive, but rather it aims to discuss PAs catalysis from another perspective. Specifically, PAs catalyzed reduction, oxidation, cross-coupling, and decomposition will be discussed in addition to other reaction types not previously mentioned.

2. Catalyzed reactions promoted by pillararenes

Modern organic synthesis is headed in the direction of controlling reaction selectivity and rate acceleration [36]. Associated with the development of new synthetic compounds is the careful design of specific catalysts. Undoubtedly, supramolecular hosts contribute enormously in this regard. The core of supramolecular catalyst design is the fundamental understanding of different factors affecting reaction outcomes. All manner of noncovalent interactions, such as hydrogen bonding, cation/anion···π interactions, C-H···π interactions, electrostatic effects, and the hydrophobic effect, *etc.*, all contribute to the energies of transition states leading to divergent reaction outcomes [37-40]. In this topic, we examine redox reactions, coupling reactions, decomposition reactions and some other unclassified reactions that are catalyzed by self-assembled pillararene architectures (Fig. 1).

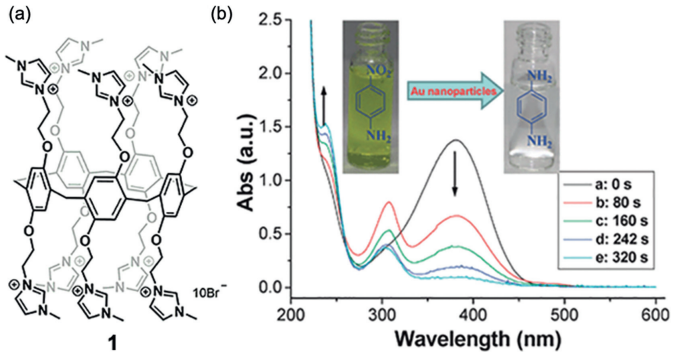

Fig. 2. (a) Structure of imidazolium functionalized P5A **1**, (b) UV–vis spectra of the reduction of 4-nitroaniline by using $NaBH_4$ and **1** stabilized AuNPs (0.08 mol%, 1.88 ± 0.58 nm) as the catalysts. Reproduced with permission [24]. Copyright 2012, Royal Society of Chemistry.

2.1. Reduction

Gold nanoparticles (AuNPs) have been exploited for the preparation of novel hybrid nanomaterials because they offer excellent stability, facile synthesis, and simple surface modifications [41,42]. Stabilizers perform a vital role in the controlled preparation and dispersion stability of AuNPs. To this ends, Huang and coworkers effectively used imidazolium functionalized P5A **1** as a stabilizer for the preparation of AuNPs [24]. The size of the AuNPs was inversely dependent on the concentration of **1**; upon addition of **1** (2–200 μmol/L), the diameter of the prepared AuNPs decreased from ~6 nm to < 2 nm. Due to the weakly coordinating shell of imidazolium and bromide (Br^-) ions around the AuNPs, the AuNPs exhibited excellent catalytic activity in the borohydride (BH_4^-) reduction of 4-nitroaniline to 1,4-diaminobenzene; while no reduction occurred in the absence of **1**. Upon addition of a small amount (0.08 mol%) of **1**, the absorption band at 400 nm of yellow colored nitroaniline diminished completely within 6 min with the concomitant increase of absorption bands at 240 nm and 300 nm, confirming the appearance of the aniline product (Fig. 2).

Zhou and Jin *et al.* [43] reported the synthesis and self-assembly of a bola-amphiphilic P5A **2**. Above the critical aggregation concentration (CAC) of ~0.4 mmol/L, **2** self-assembled into large vesicle-like multi-layered aggregates with diameters of ≥ 100 nm at near neutral pH (5–7); however, at pH ≤ 4, nanoaggregates with diameters of ~5 nm were observed corresponding to solid micelles.

The morphology of vesicles changed drastically after 4 weeks; stable microtubes formed spontaneously at pH 7. Alternatively, well-defined microtubes were formed in THF upon addition of water after mild sonication for 5 min. Furthermore, hybrid microtubes containing surface deposits of AuNPs were obtained by BH_4^- reduction of $HAuCl_4$ onto the surface of the microtubules (Fig. 3). These hybrid microtubes were employed as a recyclable catalyst for the reduction of isomeric nitrophenols in the presence of BH_4^- with yields of 95%–99% in 30 min.

Liao and Chen *et al.* [44] prepared thermoresponsive, P5A-containing, polymeric AuNP hybrid materials through reversible addition-fragmentation chain transfer (RAFT) polymerization between functionalized P5A **3** and poly(*N*-isopropylacrylamide) (PNIPAM). This was followed by subsequent chemisorption onto Citrate@AuNPs; replacement of the surface-bound citrate gave **3**@AuNPs containing a PNIPAM-trithiocarbonate linker (Fig. 4**)**, which were effectively employed as a recyclable thermoresponsive catalyst for the reduction of *p*-nitrophenol (Yield loss was < 3% after 5 catalytic cycles). The catalyst was recoverable by heating above the cloud-point of the composite (≥ 40 °C). Interestingly, the cloud point was lowered in the presence of the guest

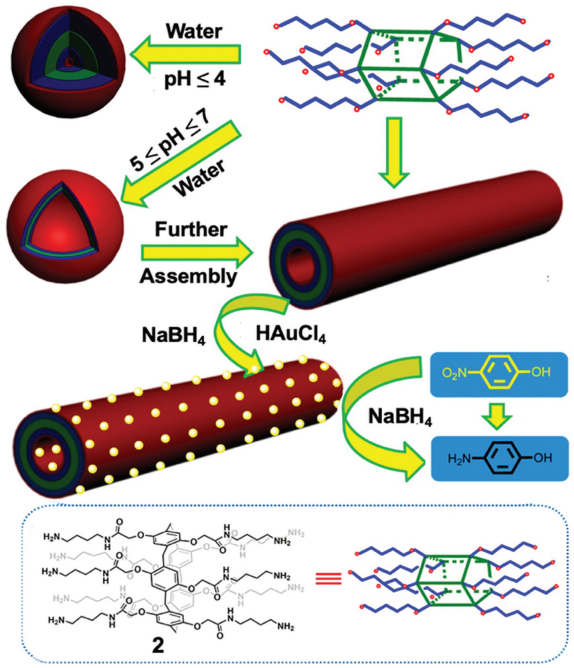

Fig. 3. Chemical structure of bola-P5A **2** and cartoon representation of the formation of different nanostructures as microreactor for reduction reactions. Reproduced with permission [43]. Copyright 2015, American Chemical Society.

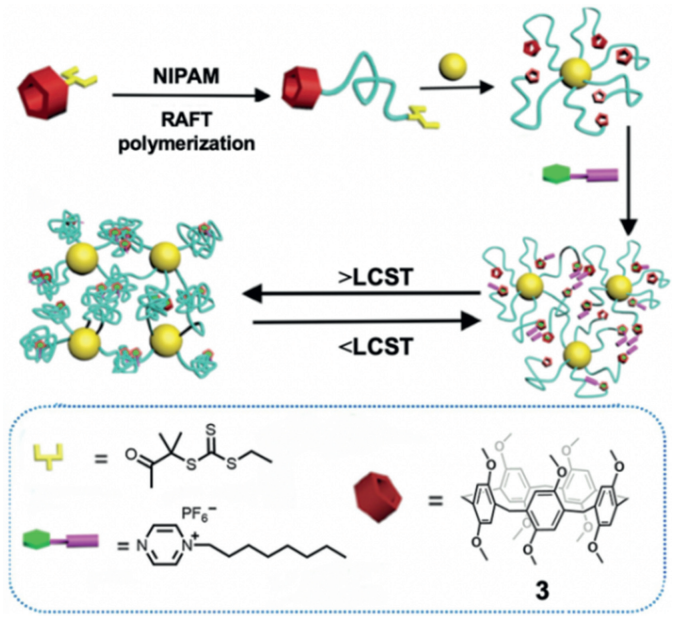

Fig. 4. Preparation of the thermoresponsive **3**-PNIPAM-AuNP hybrid materials. Reproduced with permission [44]. Copyright 2015, Wiley-VCH Verlag GmbH & Co. KGaA, Weinheim.

n-octylpyrazinium due to aggregation between the alkyl chains of *n*-octylpyrazinium and PNIPAM.

In 2019, Tan and Zhao *et al.* [45] developed a 2D heterogeneous hybrid nanomaterial consisting of 2–3 nm AuNPs dispersed within the 2D porous structure of Graphdiyne (GD). The AuNPs were prepared *in situ* with GD and P5A **4**, where **4** served to stabilize the formation of the AuNPs to give P5A **4** functionalized AuNPs that were loaded into GD (**4**@Au-GD) as shown in Fig. 5. This 2D material displayed enhanced catalytic efficiency compared to commercial Pd/C catalyst in the presence of $NaBH_4$; shorter reaction time was observed for the reduction of 4-nitrophenol and dye degradation of methylene blue (MB), 7.5 min and 5.5 min, respectively. In contrast, the Pd/C catalyzed reactions were incomplete after more than 20 min. The rate constant (k) was 11.3-fold greater for the reduction of 4-nitrophenol and 15.77-fold greater for degradation of MB compared to the Pd/C catalyst ($k = 0.042$ min^{-1}). This was ascribed to the small size distribution of the catalytically active AuNPs within the hybrid material. Due to the insolubility of the 2D catalyst, it showed high stability and recyclability without altering the size and catalytic behavior of AuNPs after five cycles. Therefore, these results revealed that porous GD materials provide a suitable coordination environment for loading of metallic NPs.

Inspired by the outstanding catalytic activities of small size AuNPs, the same group synthesized a subsequent 2D heterogeneous catalyst using P6A-reduced AuNPs within a covalent organic frameworks (COF) as a solid support (**5**@Au-COF, Fig. 6) [46]. This **5**@Au-COF material exhibited superior catalytic performance for the reduction of nitrophenol isomers compared with commercially available Pd/C catalyst. The rate constant for the reduction of 2-nitrophenol with **5**@Au-COF was up to 33-fold greater than the Pd/C catalyst; the rate enhancement was 9.05, and 5.11 times greater for 4- and 3-nitrophenol, respectively. The reduction efficiency is dependent on the porosity and crystallinity of the catalyst, which allows accumulation of the nitrophenol isomers at the surface of the COF. Additionally, electron-rich AuNPs strongly interact with the electron deficient nitrophenol isomers. These then are adsorbed onto the electron rich surface of **5**@Au-COF, which is facilitated by host–guest complexation between **5** and nitrophenol. Based on this approach, it creates an enormous number of potential close interactions between AuNPs and nitrophenol isomers. Furthermore, **5**@Au-COF did not undergo any changes in X-ray diffraction, or X-ray photoelectron spectroscopy patterns, with no loss in activity for five repetitions, demonstrating excellent recyclability and durability.

These examples have demonstrated the use of PAs employed in conjunction with AuNPs with two different solid supports, namely GD and COF, for catalyzing the reduction of nitrophenol. The synergic effect between PAs and these materials enhanced their catalytic performance, while in each instance, the stabilized AuNPs were formed with small size (approx. 3 nm) and displayed interesting sensing and self-assembly properties. The formed hybrid, heterogenous, catalytic materials are typically recyclable due to their limited solubility with little or no loss of catalytic efficiency.

2.2. Oxidation

In addition to the reductions discussed above, PA-functionalized materials have been used for photocatalytic [47] and electrocatalytic oxidation [48]. In one example, a conjugated macrocyclic polymeric (CMP) network was prepared by Sonogoshira coupling between a triflate-substituted P5A derivative **6** and tris(*p*-ethynylphenyl)triazine (Fig. 7). The CMP was used for the photocatalytic oxidation of sulfides to sulfoxides with reactant selectivity [47]. The sulfides were irradiated for 10, 20 or 30 h in open vessels; oxidation to the corresponding sulfoxides was selective for sulfides containing a linear alkyl nitrile group. Diphenyl substituted sulfides did not bind to the cavity of P5A **6** in the CMP and hence did not undergo oxidation. This was confirmed by competition experiments with butanenitrile, which effectively inhibited the formation of the sulfoxides. Another example of photooxidation of sulfide was recently achieved by Yang's group using pillararene-based multistep fluorescence-resonance energy transfer (FRET) systems [49].

Yang and Guo *et al.* employed single-walled carbon nanotubes (SWCNT) functionalized with P5A **4** to prepare hybrid nanomaterials through *in-situ* loading of AuNPs [48] (**4**@AuNPs@SWCNT, Fig. 8). The stability of the uniformly dispersed AuNPs (~10 nm) was maintained by the coordination of Au with heteroatoms of **4**

via π-π interactions and coordination bonding, improving the hydrophilicity of SWCNT. Thus, the nanomaterial exhibited excellent catalytic activity towards an ethanol oxidation reaction (EOR). During electrocatalysis the current density data showed that the peak current of **4**@AuNPs@SWCNT was approximately 1.3 times greater than **4**@AuNPs and 8 times than that of **4**@SWCNT. The superior electrocatalytic capability was attributed to uniformly dispersed SWCNT as well as to the small size of the AuNPs.

Hu and co-workers has designed an AIE (aggregation induced emission) singlet oxygen ($^1O_2$) generation system, which functioned as nanoreactors for the photooxidation of dopamine to form polydopamine with visible light irradiation (Fig. 9) [50]. This system was effective in aqueous media and was based on supramolecular host–guest assembly between a water-soluble P5A **7** and an AIE photosensitizers (TPEDM). The formed supramolecular nanoparticles exhibited significant ability to generate $^1O_2$ and displayed enhanced fluorescence. The results indicated that absorbance of the polydopamine solution only increased upon light irradiation, while the absorbance showed no significant changes in its absence. Therefore, an "ON/OFF" mode of photocatalysis was achieved.

As these examples have shown, PAs are increasingly attractive in fabricating functional materials, specifically due to their host–guest binding motifs, building strategies, topology, and ability to form stimuli-responsive networks. In regards to oxidation, PAs based synthetic macrocyclic hosts have been combined with different functionalities, such as AuNPs, SWCNTs, and photosensitizers for the facile preparation of 2D and 3D nanostructures. These PA-based nanomaterials can be employed as green electro- and photocatalysts.

2.3. Coupling reactions

One of the most useful reactions in synthetic organic chemistry are C–C bond forming or cross-coupling reactions [51]. Transition metals, especially palladium, are typically involved in these coupling reactions and can be incorporated, together with PAs, either through encapsulation or coordination. To this end, PAs and PAs based materials have been employed as effective (co)catalysts for the applications in many C–C cross-coupling reactions including the Pd-catalyzed Suzuki-Miyaura [52,53] and Heck reactions [54].

In one example using PAs based materials to catalyze a Suzuki-Miyaura cross-coupling reaction, a porous polymeric framework was obtained from P5A **3**. P5A **3** was first subjected to a Friedel-Crafts reaction with α,α'-dichloro-*p*-xylene to yield a porous polymeric framework [52]. The porous polymeric material was then oxidized with ceric ammonium nitrate ($(NH_4)_2Ce(NO_3)_5$) to a pillar[5]quinone (PQ[5]) derivative and loaded with 9.1–12.0 wt% Pd by treatment with $Pd(OAc)_2$ (Fig. 10). The Pd-loaded heterogenous catalyst (Pd-PPQ) was effective for Pd-catalyzed Suzuki-Miyaura cross-coupling reactions between aryl bromides and phenylboronic acid with yields up to 99% and high turnover frequency (up to 29,700). The catalyst was stable to elevated temperature (80 °C, 90 min) and recyclable for six cycles with essentially no change in yield.

Yao and coworkers used a P5A-based [2]rotaxane (**R**, Fig. 11) in the preparation of an organometallic cross-linked polymeric material (Pd@**R**); Pd@**R** was used as a catalyst for the Suzuki-Miyaura coupling reaction (Fig. 11) [55]. The P5A-based [2]rotaxane **R** was fabricated by threading/stopping. First, threading of perethylpillar[5]arene **8** with the aliphatic chain axle **G** occurred through host–guest complexation, which was followed by a multicomponent reaction using dimedone, malononitrile, and benzaldehyde for forming the stopper. The axle contained two triazole units which served as anchoring sites on the axle for the coordination of Pd ions after treatment of **R** with $Pd(NO_3)_2$. The obtained product

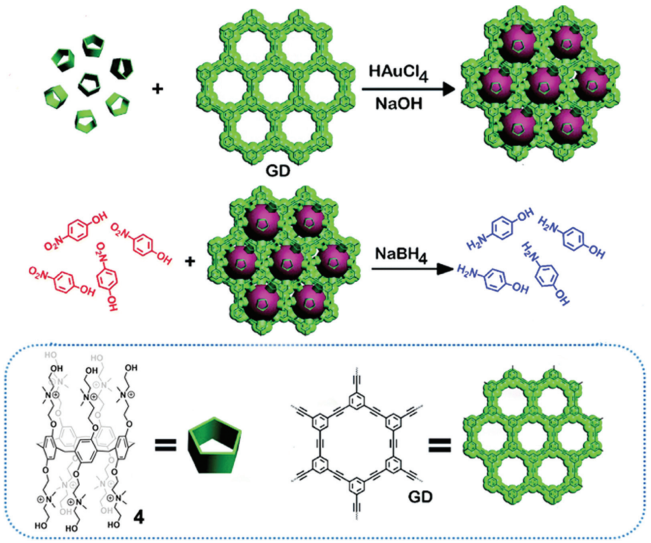

Fig. 5. Preparation of the 2D hybrid nanomaterial (**4**@Au-GD) and its catalytic reduction of nitrophenol. Reproduced with permission [45]. Copyright 2019, Royal Society of Chemistry.

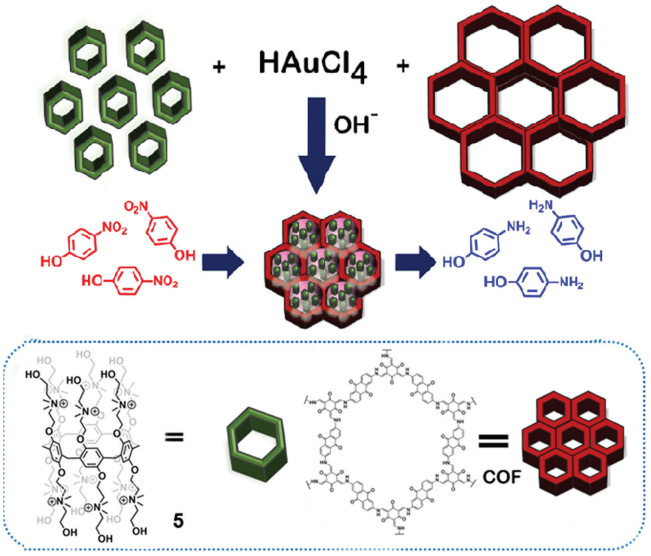

Fig. 6. Synthetic route of COF and **5**@Au-COF hybrid material and its catalytic reduction of nitrophenol isomers.

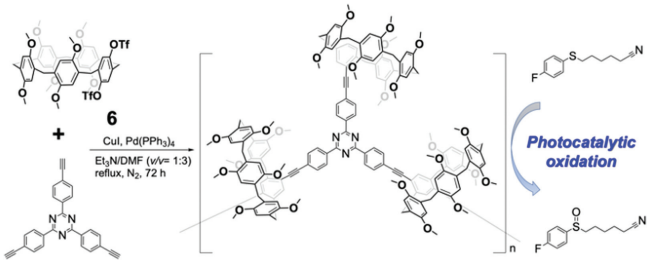

Fig. 7. PAs containing CMP used for photocatalytic reactions.

Pd@**R** showed high catalytic activity and stability with yield of 95% in the Suzuki coupling reaction. Interestingly, the Pd@**R** catalyst was reusable for three times without any loss of conversion ratio. This was attributed to the conversion of Pd(II) ions into Pd(0) particles and incorporation of Pd(0) particles into the polymeric materials after the first catalyst use. Thus, subsequent uses of the

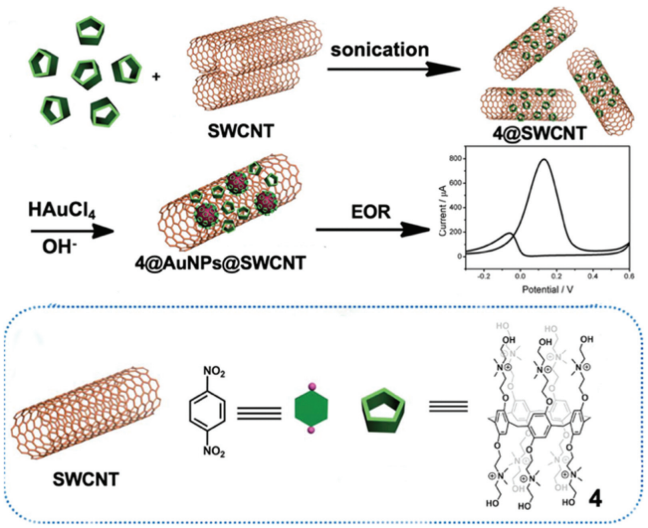

Fig. 8. The schematic representation for the preparation procedure of **4**@AuNPs@SWCNT and its application in EOR catalysis. Reproduced with permission [48]. Copyright 2019, Royal Society of Chemistry.

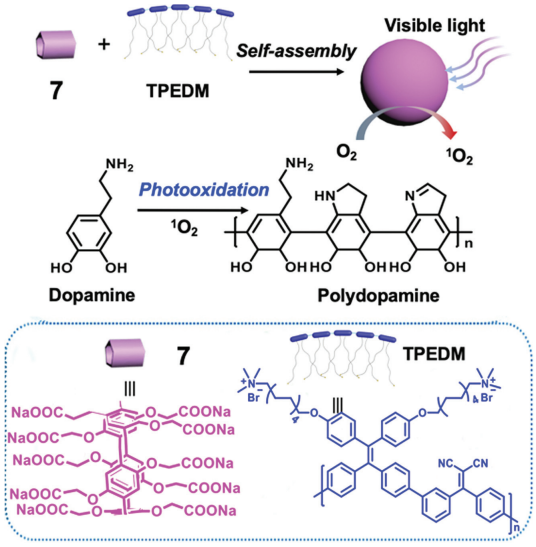

Fig. 9. Schematic representation of the supramolecular AIE chemiluminescent singlet oxygen generation system. Reproduced with permission [50], Copyright 2021, Elsevier.

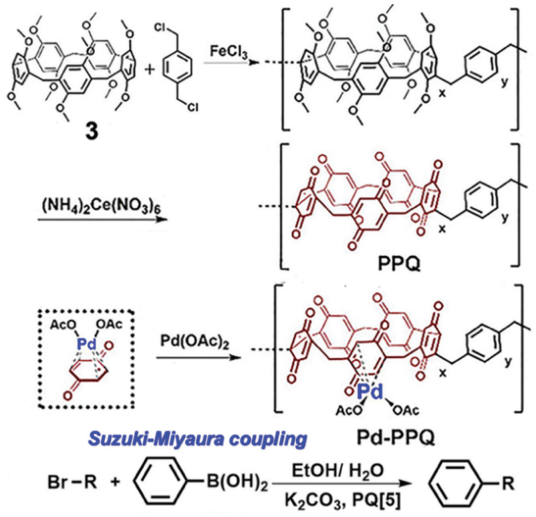

Fig. 10. Polymeric network featuring Pd-loaded pillar[5]quinones. Reproduced with permission [52]. Copyright 2019, Wiley-VCH Verlag GmbH & Co. KGaA, Weinheim.

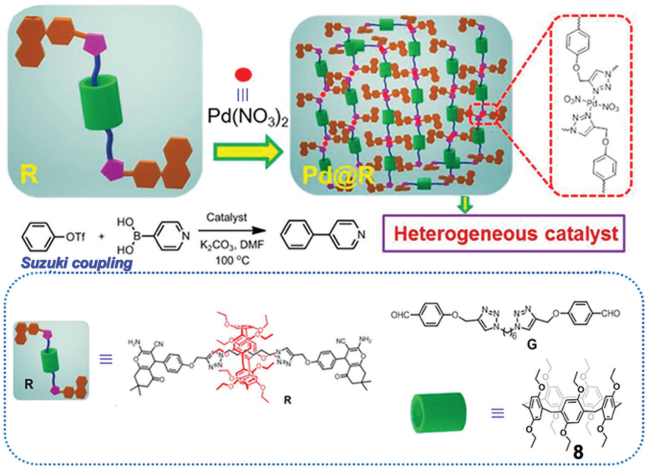

Fig. 11. Cartoon representation of the formation of Pd@**R** and its application in the coupling reaction. Reproduced with permission [55]. Copyright 2020, American Chemical Society.

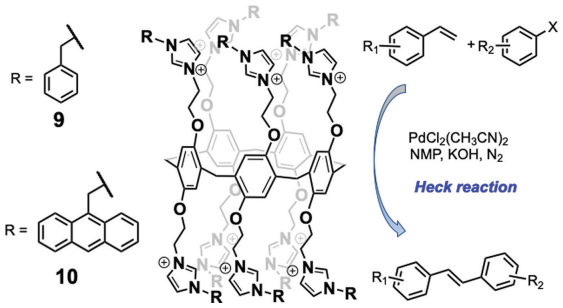

Fig. 12. Hosts **9** and **10**, and Heck coupling reaction catalyzed by hosts **9** and **10** (PF_6^- counterions not shown).

material underwent no significant changes. Furthermore, under the same conditions, Pd@**R** exhibited superior catalytic activity compared to the axle in the absence of **8**, was more readily recyclable, and was an excellent reaction carrier able to adsorb a decent proportion of substrates. Thus, the authors suggest Pd@**R** may find application in asymmetric catalysis and organic optical materials.

In another example using PAs to catalyze Suzuki reactions, Wang and coworkers employed P5A host **1** as a ligand (0.2 mol%) for Pd-catalyzed Suzuki-Miyaura cross-coupling reactions with yields up to 99% [53]. When the analogous monomer was employed at five times of the catalyst loading, an identical number of imidazolium groups were present, but, lacking a hydrophobic cavity, the yield was considerably reduced. Thus, the hydrophobic cavity was considered as an important factor in the enhanced catalytic activity in the presence of **1**. In a prior 2016 report, Wang and co-workers [54] reported two P5As that incorporated aryl imidazolium groups (**9** and **10**, Fig. 12), which can serve as *N*-heterocyclic carbene (NHC) ligands. NHC ligands have been incorporated into other macrocyclic hosts and employed extensively in supramolecular chemistry due to their excellent catalytic performance [56,57]. Thus, hosts **9** and **10** served as ligands for Pd-catalyzed Heck reactions between styrene and aryl halide derivatives. Different reactivity was observed for ligands **9** and **10**: higher yield was observed with 1.3 mol% **10** than with 2.0 mol% **9**. This was attributed to the greater steric bulk of the 1-(9-anthracenylmethyl)imidazole NHC ligand of **10**; however, control experiments (*i.e.*, reaction in the absence of host or with monomer) were not demonstrated.

To facilitate additional cross-coupling and related reactions, the combination of new or different catalysts within PAs will

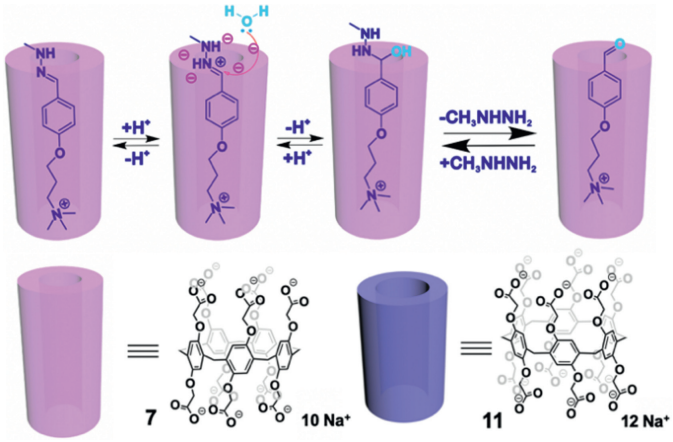

Fig. 13. Hydrolysis of hydrazones using hosts **7** and **11**. Reproduced with permission [59]. Copyright 2020, Wiley-VCH Verlag GmbH & Co. KGaA, Weinheim.

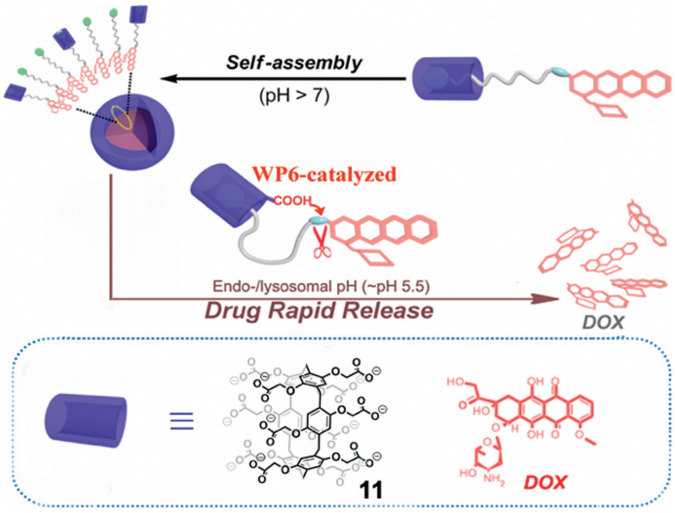

Fig. 14. DOX prodrug released under acidic conditions catalyzed by host **11**. Reproduced with permission [60]. Copyright 2015, American Chemical Society.

impart novel chemical reactivity. We anticipate the interplay between them will offer additional possibilities not only to coupling reactions but also for other organometallic chemistry. Furthermore, improved sustainability can be achieved by replacing noble metals with earth-abundant metals or by limiting catalyst loads. In many instances this can lead to a significant reduction in catalytic activity; however, this may be overcome by careful control of the system and selective modifications to facilitate enhanced reactivity and catalytic activity. As an alternative, researchers have placed extensive effort toward developing alloy NPs or core-shell NPs with earth-abundant metal cores [58]. Thus, it may be possible to replace, or minimize the consumption of noble metals for catalysis in the future with the aid of PA-based materials.

2.4. Decomposition

In contrast to reductions (Section 2.1), oxidations (Section 2.2) and cross-coupling reactions (Section 2.3), the decomposition reactions discussed in this section are generally catalyzed by PAs themselves. In this regard, the (functionalized) rims and PA cavities operate synergistically without the incorporation of other materials to effect catalysis. Sashuk and coworkers reported two catalysts based on PAs for the hydrolysis of hydrazones [59]. They prepared P5A **7** and the related P6A **11** adorned with carboxylic groups at the rims (Fig. 13). A series of hydrazones served as guests with various lengths encapsulated within **7** or **11**; different catalytic effects were dependent upon the substrate length and size of the host. The distance between the rims and the hydrazone group affected the reactivity. They also demonstrated that electrostatic stabilization of the protonated substrate accelerated the reaction, since the reaction occurred through the protonation of –CH=N– group followed by nucleophilic attack by water. Furthermore, when the PA did not possess easily ionizable groups, or no host–guest interactions were established, the reaction proceeded similarly as the blank.

Another example of P6A-catalyzed hydrazone hydrolysis was reported by Wang, Hu and coworkers for controllable drug delivery and release [60]. In their work, doxorubicin (DOX)-based prodrugs were constructed *via* an acid-cleavable hydrazone bond. The obtained prodrug could form a host–guest complex with the sodium salt of water-soluble carboxylate P6A (**11**, Fig. 14); the formed inclusion complex assembled into higher-order supramolecular nanoparticles at physiological pH (pH 7.4). Under acidic conditions (pH 5.5), the protonated carboxylate groups of **11** accelerated the cleavage of the hydrazone bond through a favored intramolecular

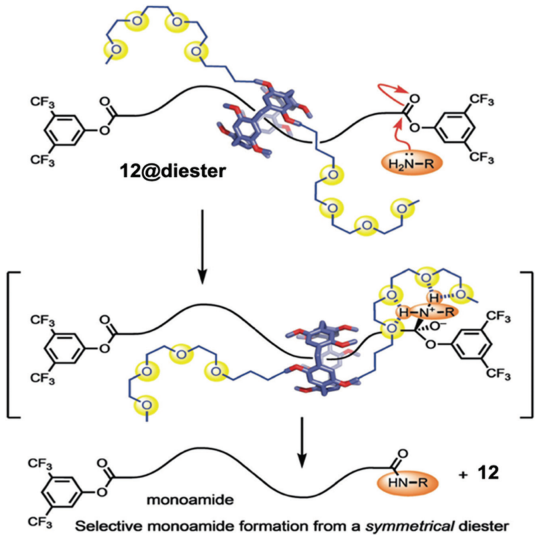

Fig. 15. Selective aminolysis of a single activated ester using **12**@diester rotaxane. Reproduced with permission [61]. Copyright 2020, from Wiley-VCH Verlag GmbH & Co. KGaA, Weinheim.

process, thus leading to rapid and almost complete release of the anticancer drug DOX.

Li and Schneebeli reported a PA-based catalytic rotaxane which was employed in selective mono aminolysis [61]. They prepared four P5A-based catalytic rings, which were appended with catenanes spaced by CH_2 linkers, P[5]cat-C*n*, ($n = 0$, 2, 4, or 8) where *n* represents the number of CH_2 groups. They determined the C4 linker (12, Fig. 15) placed optimal distance between the two catenane moieties on the monoester rotaxane prepared from (3,5 bis(trifluoromethyl)phenoxy)hexadecanoyl chloride (axle) and 3,5-bis(trifluoromethylphenol) (stopper). The catalytic efficiency increased with the length of the linker from P[5]cat-C0 to P[5]cat-C4 (**12**), which consequently led to the formation of the most catalytically active 4-Coord intermediates during aminolysis. The unique interlocked structure contained a catalytic ring, controlling the reactivity of the ester groups. In the presence of **12**@diester, the monoamide formed in 74% yield, compared to a maximal 32% yield in the absence of the catenane appendages. Furthermore, **12** could be used to distinguish between two very similar dimethyl phenols by first transesterification of the blocking groups and subsequent

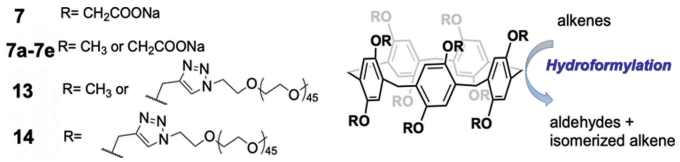

Fig. 16. Chemical structures of P5As **7**, **7a-7e**, **13**, and **14**, and their applications in hydroformylation.

treatment of the mixture with *n*-butylamine; the 3,5-disubstitued phenol selectively underwent aminolysis in the presence of the 3,4-disubstituted phenol.

To further control reactivity and product selectivity, future development of PAs is required. Modifications to the rim to enhance solubility in desired media can have the added effect of offering additional means of incorporating one or more functional groups (*e.g.*, amino acid residues) to develop *de novo* enzymatic pockets. Furthermore, to promote more complicated catalysis that allows for larger or multiple reactants, larger PA homologues are required while extended cavities will allow bimolecular reactions of greater substrate scope and complexity. For example, Ogoshi reported cavitand-like PAs derived from per-hydroxylated P6A; the extended cavity was constructed by bridging the hydroxyls of adjacent hydroquinone units with dialkyldichlorosilanes in an alternating up-and-down motif [62]. They also demonstrated length-controlled discrete tubular structures by homo-/co-assembly of rim-differentiated and peralkylamino P5As *via* hydrogen bonds and salt bridges [63].

2.5. Other reaction types

Recently, a collaboration between Potier and Hapiot [64] produced P5A akin to **7** (Fig. 9) but with some of the carboxylates substituted by methyl groups. Thus, either methyl or sodium methyl carboxylate groups are present (*i.e.*, P5A-$(Me)_{10-x}$-$(CH_2COONa)_x$, with x being the number of sodium methyl carboxylate groups distributed on both sides of the macrocycle, **7a-7e**, Fig. 16). These hosts served as interfacial additives in aqueous biphasic catalysis. Surface tension measurements revealed that the modified P5As adsorbed differently at the air/aqueous interface dependent upon the degree of substitution. The modified P5As were investigated for their performance in rhodium (Rh)-catalyzed hydroformylation of 1-decene and 1-hexadecene. The conversion of 1-decene increased to a maximum of 85% (72% for 1-hexadecene) with increasing number of sodium carboxylates (x) up to *ca.* 8, then lowered for greater carboxylate substitution; the additional carboxylates likely reduced the affinity of the substrate and catalyst, leading to decreased conversion. Thus, a fine balance of carboxylate and methyl groups was critical to ensure adsorption at the biphasic interface and molecular recognition of the guest. The investigated P5As showed lower chemoselectivity, similar catalytic activity, and higher regioselectivity when compared to other interfacial additives such as modified cyclodextrins. Derivatives containing either five polyethylene glycol (PEG) chains and five methyl groups (**13**), or ten PEG chains (**14**) exhibited better conversion and selectivity due to their ability to partition organic substrates within the aqueous biphasic system. However, use of persubstituted **14** had a detrimental effect on both the conversion percent and aldehyde selectivity compared to **13**; one plausible explanation was the recognition of the substrate within the cavity was hampered by the bulky PEG-triazolylmethyl moieties.

The P5A based [1]rotaxane **15** was used as a catalyst for Knoevenagel condensation (Fig. 17) [65]. The synthesis of **15** was achieved by aminolysis of a prepared monoester at one rim, followed by direct capping of the formed amino-terminated pseudo[1]rotaxane *via* an S_N2 reaction with 1-(bromomethyl)-3,5-

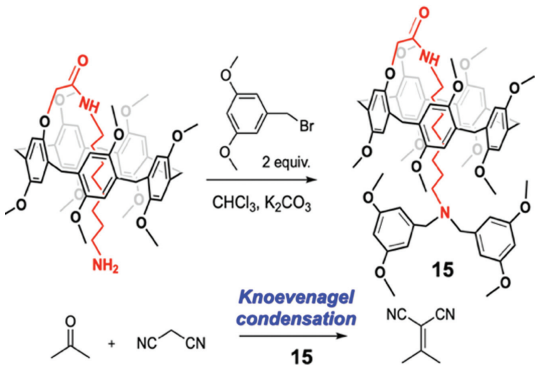

Fig. 17. Knoevenagel condensation catalyzed by **15**. Reproduced with permission [65]. Copyright 2017, the Royal Society of Chemistry.

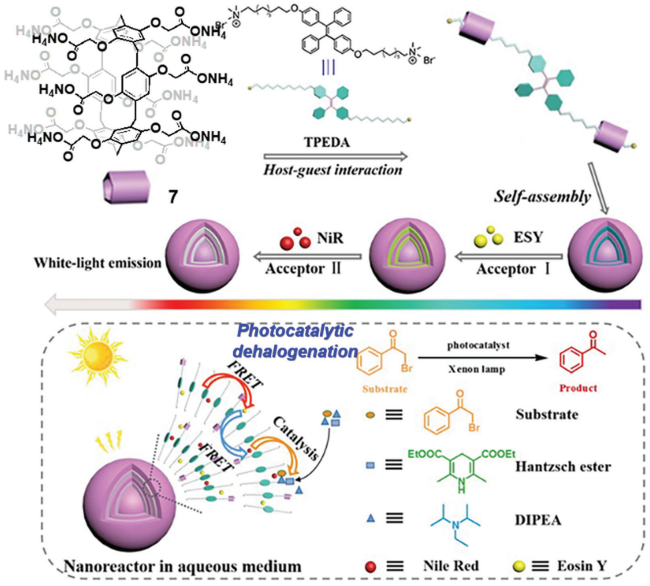

Fig. 18. Photocatalytic dehalogenation catalyzed by pillararene **7** based FRET system. Reproduced with permission [31]. Copyright 2019, Wiley-VCH Verlag GmbH & Co. KGaA, Weinheim.

dimethoxybenzene as a stopper. The rotaxane **15** bears a tertiary amine group that functions as a weak organic base. In the absence of any catalyst, the condensation reaction between acetone and malononitrile did not occur at room temperature, but the reaction proceeded smoothly and followed second order kinetics in the presence of **15**. Although **15** did not show any advantages over the analogous monomeric tertiary amine, and the space effect of P5A hindered catalysis, this work represents the first example of supramolecular catalysis with a P5A-based [1]rotaxane.

Other reaction types not previously discussed are also possible with PAs based catalysis. One electrochemical example involving P5A **1** was reported by Chen *et al.* They employed the MoS_2/reduced graphene oxide (rGO) hybrid nanomaterials (**1**@MoS_2/rGO) as a electrocatalyst for hydrogen evolution reaction [66]. Besides, radical reaction can be performed efficiently by pillararene-based architecture. For instance, Chang's group reported that pillar[6]arene can be used to initiate free-radical photopolymerization [67]. Hu and co-workers focused on using water-soluble pillararene assembled FRET systems to catalyze dehalogenation reaction [68]. In details, a water-soluble artificial light-harvesting system with sequential energy transfer process was fabricated through supramolecular self-assembly of water-soluble pillar[5]arene (ammonium salt of **7**), bola-type tetraphenylethlene-

modified dialkylammonium derivatives (TPEDA) and fluorescent dyes, NiR and ESY (Fig. 18) [31]. The harvested energy of the system with two-step energy transfer process could be further employed for dehalogenation of α-bromoacetophenone in water with yield up to 96% compared with the control group using organic dyes alone.

3. Conclusions

PAs are macrocyclic host molecules whose increasing popularity in catalysis is driven by their inherent versatility, flexibility, and capability to readily synthesize specific variations at the peripheral functional groups surrounding the aromatic core. Thus far, the focus has been on P5As and P6As, however, as larger homologues become more readily available through improved synthetic strategies, their popularity will continue to expand. Further post-synthetic modifications will lead to specific host–guest complexations, which may be fine-tuned to particular catalytic applications. In this review, we have summarized the recent advances in PAs based catalysis, which is a relatively less explored field compared to other applications such as sensors, separations and drug delivery; however, this field has seen gradual increasing publications in recent years. As discussed, PAs have been employed in catalyzing various types of reactions including reductions, oxidations, coupling reactions, and decompositions among others. Although PAs are used as successful catalysts for many different reaction types, only a small fraction of possible chemical reactions has been examined. As different catalytic mechanisms are elucidated, more efficient enzyme-like reaction examples will be developed.

While interest in using PAs architectures to catalyze reactions has grown rapidly, there are still challenges that await ahead to be conquered. The synergy should be established between substrate conformation inside PAs cavity and how the cavity is used to stabilize the transition states. Further understanding of interaction between PAs and different functionalities is also crucial in expanding the catalyzed reaction types and bringing unique reactivity. Future development of PAs based catalysis can be explored by (i) modifications to the rim or expansion of the PA cavity, and (ii) by incorporating different functionalities to form macromolecular structures (*e.g.*, vesicle, sheet or tube). In the first instance the catalytic activity is controlled only by the synthetic design of the PAs and their attached pendent groups, which will offer more interactions with substrates, while in the second, the combination of different moieties such as metallic ions, nanoparticles, or other organic molecules with PAs leads to their catalytic activity. By taking advantage of either covalent linkages and conjugation or supramolecular assembly, a plethora of different structures can be explored. We envision more complicated and exquisite PA architectures will be constructed in the future.

Declaration of competing interest

There are no conflicts to declare.

Acknowledgments

This work was supported by the Natural Science Foundation of Jiangsu Province (No. BK20200432), National Natural Science Foundation of China for Sino-German Mobility Program (No. M-0411), and the Fundamental Research Funds for the Central Universities (Nos. NE2019002 and NS2021040). We thank Dr. Makesh Mohan for designing the TOC graphic image.

References

[1] A. Stank, D.B. Kokh, J.C. Fuller, R.C. Wade, Acc. Chem. Res. 49 (2016) 809–815.
[2] X. Liu, K. Wang, M. Externbrink, et al., Chin. Chem. Lett. 31 (2020) 1239–1242.
[3] C.A. Strulson, R.C. Molden, C.D. Keating, P.C. Bevilacqua, Nat. Chem. 4 (2012) 941–946.
[4] R.J. Peters, M. Marguet, S. Marais, et al., Angew. Chem. Int. Ed. 53 (2014) 146–150.
[5] A.B. Grommet, M. Feller, R. Klajn, Nat. Nanotech. 15 (2020) 256–271.
[6] X. Hu, Z. Pei, Chin. Chem. Lett. 29 (2018) 1703–1705.
[7] K. Wang, J. Jordan, X.Y. Hu, L. Wang, Angew. Chem. Int. Ed. 59 (2020) 13712–13721.
[8] C.J. Brown, F.D. Toste, R.G. Bergman, K.N. Raymond, Chem. Rev. 115 (2015) 3012–3035.
[9] Y. Fang, J.A. Powell, E. Li, et al., Chem. Soc. Rev. 48 (2019) 4707–4730.
[10] T. Ogoshi, S. Kanai, S. Fujinami, T.A. Yamagishi, Y. Nakamoto, J. Am. Chem. Soc. 130 (2008) 5022–5023.
[11] T. Ogoshi, T.A. Yamagishi, Y. Nakamoto, Chem. Rev. 116 (2016) 7937–8002.
[12] M. Xue, Y. Yang, X. Chi, Z. Zhang, F. Huang, Acc. Chem. Res. 45 (2012) 1294–1308.
[13] N.L. Strutt, H. Zhang, S.T. Schneebeli, J.F. Stoddart, Acc. Chem. Res. 47 (2014) 2631–2642.
[14] K. Jie, Y. Zhou, E. Li, F. Huang, Acc. Chem. Res. 51 (2018) 2064–2072.
[15] T. Ogoshi, T. Kakuta, T.A. Yamagishi, Angew. Chem. Int. Ed. 58 (2019) 2197–2206.
[16] T. Kakuta, T.A. Yamagishi, T. Ogoshi, Acc. Chem. Res. 51 (2018) 1656–1666.
[17] N. Song, T. Kakuta, T.A. Yamagishi, Y.W. Yang, T. Ogoshi, Chem 4 (2018) 2029–2053.
[18] W. Feng, M. Jin, K. Yang, Y. Pei, Z. Pei, Chem. Commun. 54 (2018) 13626–13640.
[19] S. Fa, T. Kakuta, T.A. Yamagishi, T. Ogoshi, CCS Chem. 1 (2019) 50–63.
[20] H. Zhang, Z. Liu, Y. Zhao, Chem. Soc. Rev. 47 (2018) 5491–5528.
[21] J. Chen, Y. Wang, C. Wang, et al., Chem. Commun. 55 (2019) 6817–6826.
[22] J.D. Ding, W.J. Jin, Z. Pei, Y. Pei, Chem. Commun. 56 (2020) 10113–10126.
[23] T. Ogoshi, N. Ueshima, T.A. Yamagishi, Org. Lett. 15 (2013) 3742–3745.
[24] Y. Yao, M. Xue, X. Chi, et al., Chem. Commun. 48 (2012) 6505–6507.
[25] Y. Yao, M. Xue, Z. Zhang, et al., Chem. Sci. 4 (2013) 3667–3672.
[26] D.G. Liz, A.M. Manfredi, M. Medeiros, et al., Chem. Commun. 52 (2016) 3167–3170.
[27] E.H. Wanderlind, D.G. Liz, A.P. Gerola, et al., ACS Catal. 8 (2018) 3343–3347.
[28] N. Cheng, Y. Chen, X. Wu, Y. Liu, Chem. Commun. 54 (2018) 6284–6287.
[29] M. Zeng, K. Chen, J. Tan, J. Zhang, Y. Wei, Front. Chem. 6 (2018) 457.
[30] Y. Sun, F. Guo, T. Zuo, J. Hua, G. Diao, Nat. Commun. 7 (2016) 12042.
[31] M. Hao, G. Sun, M. Zuo, et al., Angew. Chem. Int. Ed. 15 (2019) 10095–10100.
[32] Z. Li, X. Li, Y.W. Yang, Small 15 (2019) e1805509.
[33] Y. Liu, B. Lou, L. Shangguan, et al., Macromolecules 51 (2018) 1351–1356.
[34] R. Zhang, X. Yan, H. Guo, et al., Chem. Commun. 56 (2020) 948–951.
[35] K. Wang, J. Jordan, K. Velmurugan, et al., Angew. Chem. Int. Ed. 60 (2021) 9205–9214.
[36] F.D. Toste, M.S. Sigman, S.J. Miller, Acc. Chem. Res. 50 (2017) 609–615.
[37] K. Wang, X. Cai, W. Yao, et al., J. Am. Chem. Soc. 141 (2019) 6740–6747.
[38] Q. Zhang, K. Tiefenbacher, Nat. Chem. 7 (2015) 197–202.
[39] D.M. Kaphan, M.D. Levin, R.G. Bergman, K.N. Raymond, F.D. Toste, Science 50 (2015) 1235–1238.
[40] Y. Yu, J. Rebek Jr., Acc. Chem. Res. 51 (2018) 3031–3040.
[41] K. Saha, S.S. Agasti, C. Kim, X. Li, V.M. Rotello, Chem. Rev. 112 (2012) 2739–2779.
[42] H. Jans, Q. Huo, Chem. Soc. Rev. 41 (2012) 2849–2866.
[43] R. Chen, H. Jiang, H. Gu, et al., Org. Lett. 17 (2015) 4160–4163.
[44] X. Liao, L. Guo, J. Chang, et al., Macromol. Rapid Commun. 36 (2015) 1492–1497.
[45] X. Tan, J. Xu, T. Huang, et al., RSC Adv. 9 (2019) 38372–38380.
[46] X. Tan, W. Zeng, Y. Fan, J. Yan, G. Zhao, Nanotechnology 31 (2020) 135705.
[47] H. Qiang, T. Chen, Z. Wang, et al., Chin. Chem. Lett. 31 (2020) 3225–3229.
[48] T. Borjigin, G. Zhao, Y. Zhang, et al., Sustain. Energ. Fuels 3 (2019) 2312–2320.
[49] P.P. Jia, L. Xu, Y.X. Hu, et al., J. Am. Chem. Soc. 143 (2021) 399–408.
[50] M. Zuo, W. Qian, M. Hao, et al., Chin. Chem. Lett. 32 (2021) 1381–1384.
[51] A. Biffis, P. Centomo, A. Del Zotto, M. Zecca, Chem. Rev. 118 (2018) 2249–2295.
[52] S. Lan, X. Yang, K. Shi, R. Fan, D. Ma, ChemCatChem 11 (2019) 2864–2869.
[53] X.D. Xiao, J.Q. Liu, Y.L. Bai, R.H. Wang, J.W. Wang, J. Inclusion Phenom. Macrocyclic Chem. 87 (2016) 29–36.
[54] X.D. Xiao, Y.L. Bai, J.Q. Liu, J.W. Wang, Tetrahedron Lett. 57 (2016) 3385–3388.
[55] H. Guo, J. Ye, Z. Zhang, et al., Inorg. Chem. 59 (2020) 11915–11919.
[56] A.R. Davalos, E. Sylvester, S.T. Diver, Organometallics 38 (2019) 2338–2346.
[57] M. Poyatos, J.A. Mata, E. Peris, Chem. Rev. 109 (2009) 3677–3707.
[58] D. Sardar, M. Sengupta, A. Bordoloi, et al., Appl. Surf. Sci. 405 (2017) 231–239.
[59] S. Kosiorek, N. Rad, V. Sashuk, ChemCatChem 12 (2020) 2776–2782.
[60] Y. Cao, Y. Li, X.Y. Hu, et al., Chem. Mater. 27 (2015) 1110–1119.
[61] S.C. Rajappan, D.R. McCarthy, J.P. Campbell, et al., Angew. Chem. Int. Ed. 59 (2020) 16668–16674.
[62] T. Ogoshi, K. Demachi, K. Masaki, T.A. Yamagishi, Chem. Commun. 49 (2013) 3952–3954.
[63] S. Fa, Y. Sakata, S. Akine, T. Ogoshi, Angew. Chem. Int. Ed. 59 (2020) 9309–9313.
[64] M. Benatmane, K. Cousin, N. Laggoune, et al., ChemCatChem 10 (2018) 5306–5313.
[65] X.S. Du, C.Y. Wang, Q. Jia, et al., Chem. Commun. 53 (2017) 5326–5329.
[66] Z. Yu, J. Ye, W. Chen, S. Xu, Mater. Lett. 188 (2017) 48–51.
[67] S. Zhao, T. Xue, D. Pei, et al., Org. Lett. 23 (2021) 1709–1713.
[68] G. Sun, M. Zuo, W. Qian, et al., Green Synth. & Catal. 2 (2021) 32–37.